# Analysis of a Multilevel Voltage-Based Coordinating Controller for Solar-Wind Energy Generator: A Simulation, Development and Validation Approach

Thilagawathy Lachumanan
Faculty of Electronics and Computer Engineering
Universiti Teknikal Malaysia Melaka
Melaka, Malaysia
thilagaa1@hotmail.com

Ranjit Singh Sarban Singh
Advanced Sensors and Embedded Controls
Centre for Telecommunication Research and Innovation
Faculty of Electronics and Computer Engineering
Universiti Teknikal Malaysia Melaka
Melaka, Malaysia
ranjit.singh@utem.edu.my

Mohd Ibrahim Shapiai
Centre of Artificial Intelligence and Robotic iKohza
Malaysia – Japan International Institute of Technology
Universiti Teknologi Malaysia
Kuala Lumpur, Malaysia
md_ibrahim83@utm.my

T. Joseph Sahaya Anand
Faculty of Mechanical and Manufacturing Engineering Technology
Universiti Teknikal Malaysia Melaka
Melaka, Malaysia
anand@utem.edu.my

**Abstract-This paper presents the development and the performance analysis of the developed model of a voltage-based coordinating controller. This model is developed to perform activities such as sensing, measuring, switching, coordinating, and effectively managing the output voltages produced by the solar-wind renewable energy sources in order to supply the connected load or/and charge the battery storage system. The developed model has different tasks to perform when solar-wind energy sources both produce output voltages simultaneously, also contributing to solving the requirements of different synchronization algorithms for a multi-agent renewable energy system. The sensed and measured output voltages of the solar-wind energy sources are used as directive information to allow the developed model's controller to supply the available power to the connected load or/and charge the battery storage system. Also, the produced information at the model's controller input is used to individually control the other sub-system, which directly assists in achieving the aim of simultaneous operation when both solar and wind energy sources produce output voltages. The model is developed and simulated in Matlab/Simulink. The simulation results are used to validate the developed methodology and the aims of the developed model.**

***Keywords-voltage-based; coordinating controller; renewable energy sources; Matlab/Simulink; solar-wind***

## I. INTRODUCTION

Irregularity of energy production and generation by Renewable Energy Sources (RESs) [1] makes it necessary for the microgrid system to integrate an energy storage system to stabilize the overall performance of the DC-based microgrid systems [2-5]. Reviewing the evolution of DC-based microgrid systems [6] and their complexity, Energy Management Systems (EMSs) [7-12] have been introduced. The EMS technology for microgrid-based systems is divided into two categories: (i) Centralized EMS (CEMS) [8] and (ii) Decentralized EMS (DEMS) [12]. A CEMS is also known as the AC-based system, a microgrid connected to a transmission grid while the DEMS is a DC-based system where the microgrid is a standalone system.

Systems that have employed the EMSs into the Distributed Generation (DG) sources such as solar photovoltaic (PV) panels [13], wind turbine systems [14], hydropower systems [15], etc., into DC-based microgrid systems provide a reliable solution able to supply electrical power to rural communities where the national grid is not reachable [16]. Systems proposed in [8, 17, 18] deploy a centralized agent which transfers and shares information and electricity with the other agents' controllers. The other agents are RESs, the grid network, load consumption, and the battery storage system. The centralized agent acts as the master, and it is responsible for managing the data and sending the action to agents based on the real-time information. In [9], the decentralized multi agent was introduced. Each agent in the proposed system works by receiving information through sensors. The disadvantage of this method is that each agent has its own algorithm and needs to be synchronized with complicated coding. Authors in [19] suggested a voltage divider switching technique as the sensing and measuring of output voltages of RESs. The voltage divider switching configuration is proposed for self-intervention of a hybrid renewable energy system.

Corresponding author: Ranjit Singh Sarban Singh

The disadvantage found in [9] and the advantage of having EMS DC-based microgrid systems for the rural communities encouraged the development of the VBCC (Voltage-Based Coordinating Controller) model for the DC-based solar-wind RES microgrid system. With the development of VBCC, a single mechanism was used instead of different algorithms for each agent. In terms of contribution, the developed VBCC can strategically contribute, control, and manage the connected sources via its multilevel voltage sensing and measurement mechanism. Besides that, the integration of multilevel voltage sensing reduces the impact on the system, when the voltage is low. The voltage is used to charge the battery energy storage and at the same time discharge the battery to the connected load.

The proposed VBCC senses, measures, coordinates, controls, and effectively manages the output voltages from the distributed generators for the connected load and charge battery energy system.

## II. SYSTEM COMPONENTS

The developed VBCC consists of:

- Electronic Stateflow Condition Circuit (ESCC)
- Electronic Logic "AND" Gate Circuit (ELGC)
- Electronic Conditions Switching Circuit (ECSC)
- DC Boost Converter (DC-BC)
- Current Conversion Circuit (CCC)

The VBCC is responsible for sensing, measuring, coordinating, switching, and effectively managing the generated energies from solar-wind RESs which generate output simultaneously while performing different roles when the VBCC is operating. Figure 1 shows the modeled block diagram of the integrated VBCC. Solar energy is produced from solar PV panels and wind energy is produced from a wind turbine generator as shown in Figure 1.

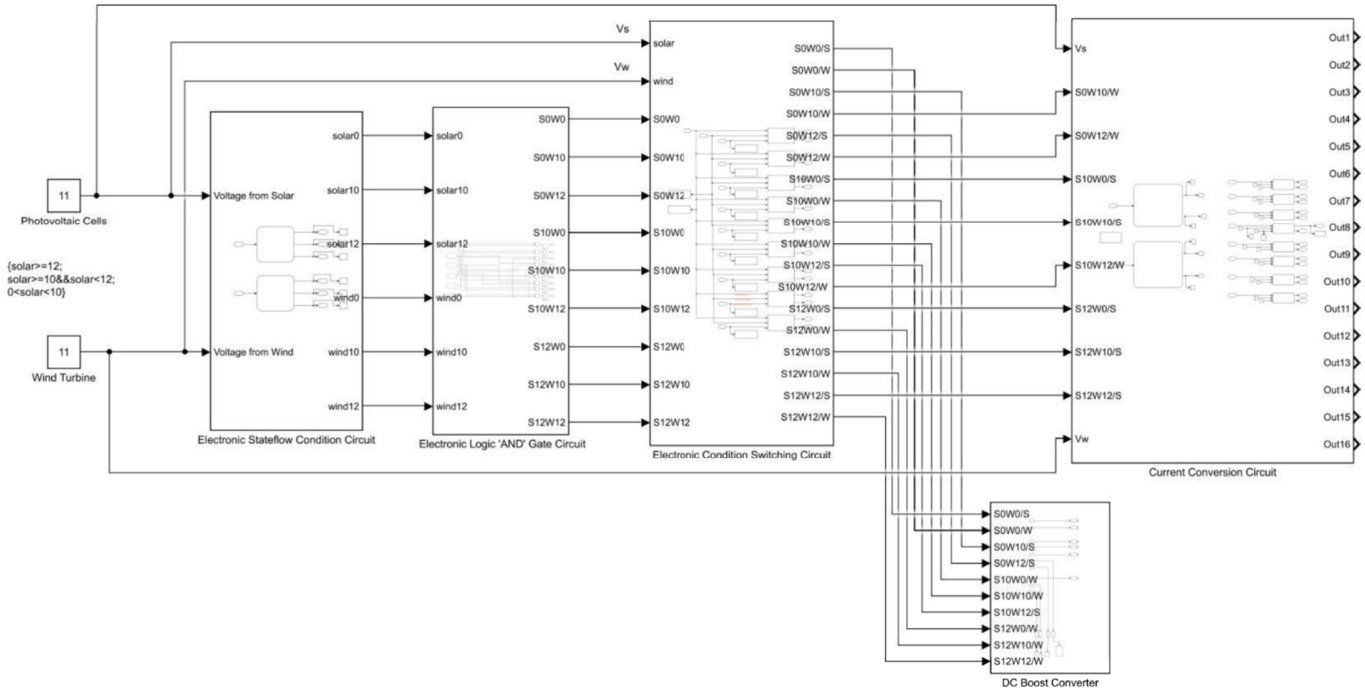


Fig. 1. The VBCC developed model.

TABLE I. SOLAR-WIND GROUPED CONDITIONS

| No. | Grouped conditions |
|---|---|
| 1 | $0V \leq V_{solar} < 10V$ and $0V \leq V_{wind} < 10V$ |
| 2 | $0V \leq V_{solar} < 10V$ and $10V \geq V_{wind} > 12V$ |
| 3 | $0V \leq V_{solar} < 10V$ and $12V \geq V_{wind} \geq 15V$ |
| 4 | $10V \geq V_{solar} > 12V$ and $0V \leq V_{wind} < 10V$ |
| 5 | $10V \geq V_{solar} > 12V$ and $10V \geq V_{wind} > 12V$ |
| 6 | $10V \geq V_{solar} > 12V$ and $12V \geq V_{wind} \geq 15V$ |
| 7 | $12V \geq V_{solar} \geq 15V$ and $0V \leq V_{wind} < 10V$ |
| 8 | $12V \geq V_{solar} \geq 15V$ and $10V \geq V_{wind} > 12V$ |
| 9 | $12V \geq V_{solar} \geq 15V$ and $12V \geq V_{wind} \geq 15V$ |

The solar and wind stateflow condition charts are categorized into 3 divisions which are:

- $0 \text{ Volt} \leq VR < 10 \text{ Volt}$
- $10 \text{ Volt} \leq VR < 12 \text{ Volt}$
- $12 \text{ Volt} \leq VR \leq 15 \text{ Volt}$

where R is the solar or wind RESs shown in Figure 1. The ranges of output voltages for the solar – wind RESs are summarized in Table I.

## III. WORKING PRINCIPLE OF THE COMPONENTS OF THE VBCC SYSTEM

### *A. Electronic Stateflow Condition Circuit (ESCC)*

The ESCC senses the total output analogue voltage amount of the individual solar - wind RES based on the primary division voltage ranges shown in Figure 2. For example, if the solar source produces voltage 9V and the wind produces 9V, then solar10 and wind10 in Figure 2 will produce a logic 1. This logic 1 then will be sent into the electronic logic "AND" gate circuit.

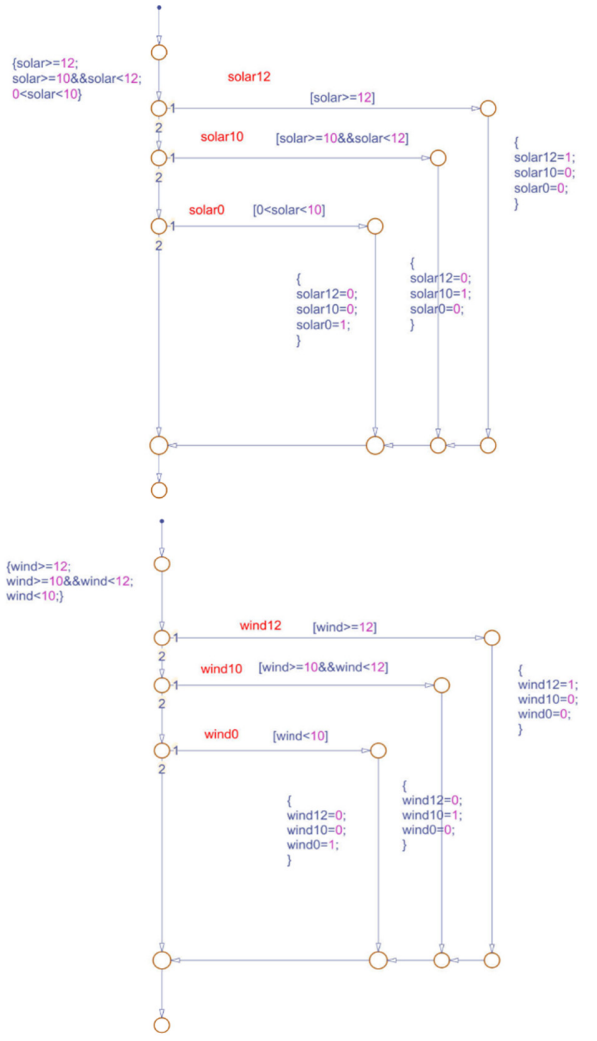


Fig. 2. Solar – wind primary voltage division ranges.

### *B. Electronic* Logic "AND" Gate Circuit (ELGC)

The ELGC is combinational of 9 AND gates and is shown in Figure 3. Each of the 9 AND gates takes an individual logic from each primary division range from the ESCC shown in Figure 2. The 2 inputs of the AND gate produce a single logic output which is used to switch ON any respective switching circuit in the electronic conditions switching circuits shown in Figure 1. When solar0 and wind0 are equal to logic 1, the S0W0 outputs a logic 1 too. The S10W10 logic 1 is sent to switch ON S10W10 of electronic conditions switching circuits. The other combinational AND gate circuits also have their decision-making roles based on the combinational input logics from the stateflow condition charts of solar – wind primary voltage division ranges.

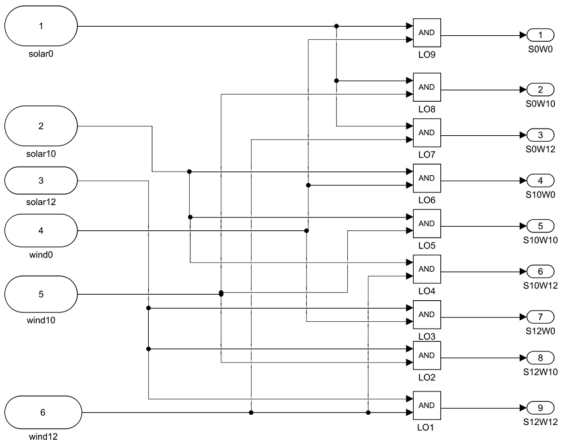


Fig. 3. The 9 AND gate combinational circuit.

### *C. Electronic* Conditions Switching Circuit (ECSC)

The ECSC of 9 conditional switching circuits is shown in Figure 4(a). Figure 4(b) shows the S10W10 condition switching circuit which is integrated as one conditional switching circuit in Figure 4(a). The S10W10 output logic 1 mentioned in Section B is sent into S10W10 of the conditional switching circuit of electronic conditions switching circuit in Figure 4(a). The S10W10 logic 1 then turns ON the relays shown in Figure 4(b). When the relays are turned ON, the output from the switches is sent to the SPDT relays to turn ON the SPDT relays from Normally Open (NO) to Normally Closed (NC). When the SPDT relays are at NC, the solar and wind input voltages are connected to S10W10/S and S10W10/W as shown in Figure 1. The S10W10/S and S10W10/W will output voltages in the range of 10V to 12V to next respective system component.

### *D. DC Boost Converter*

The Direct Current (DC) Boost Converter (BC) is shown in Figure 5. In an explained example, the S10W10/S and S10W10/W will output voltage of 10V to 12V. Then the output voltage of S10W10/W is connected to S10W10/W. The 10V to 12V from S10W10/W is sent into the DC-BC Input as shown in Figure 6. The DC_BC Output will output an increased voltage compared to the input voltage at the DC_BC Input. The increased voltage output at the DC_BC Output is used to perform the battery energy system charging process as shown in Figure 5.

(a)

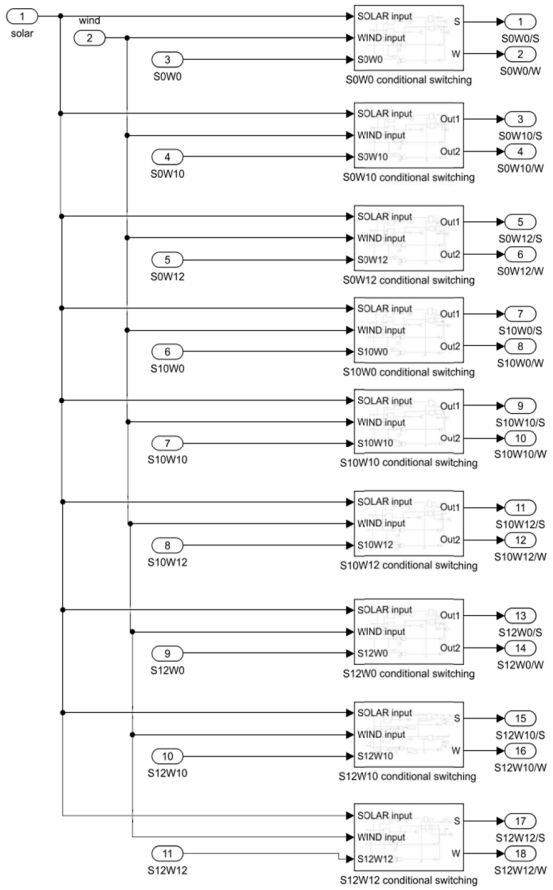


(b)

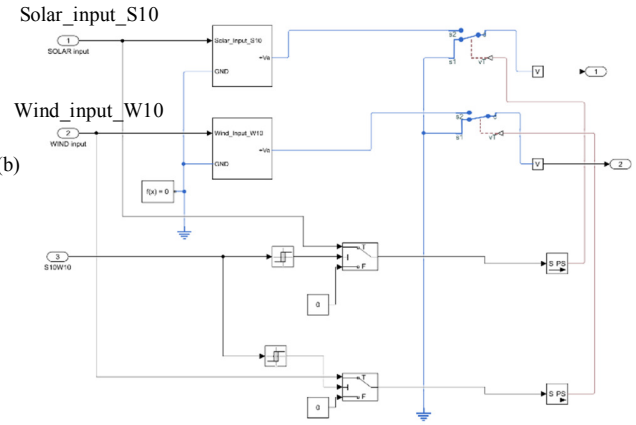


Fig. 4. (a) 9 conditional switching circuits, (b) S10W10 condition switching circuit.

The S10W10/S will output voltage between 10V and 12V which is sent into S10W10/S as shown in Figure 1. The input 10V-12V at S10W10/S is sent into the S10W10/S input shown in Figure 7. From there, it is sent to the DC BC at both Voltage inputs as shown in Figure 8. But only one DC BC is activated which is the volt10 DC BC. Logic 1 of S10W10/S is sent into volt10 port to switch the SPDT relay from NO to NC and allow the 10V to 12V incoming voltage to be increased.

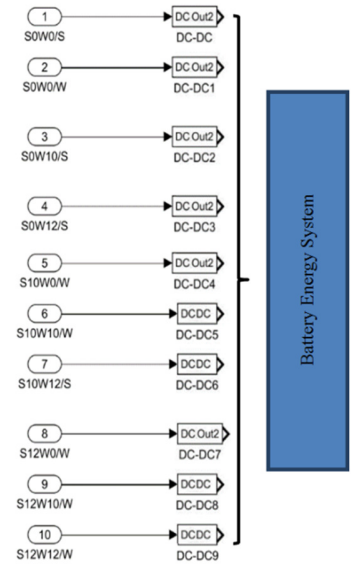


Fig. 5. DC – DC boost converters.

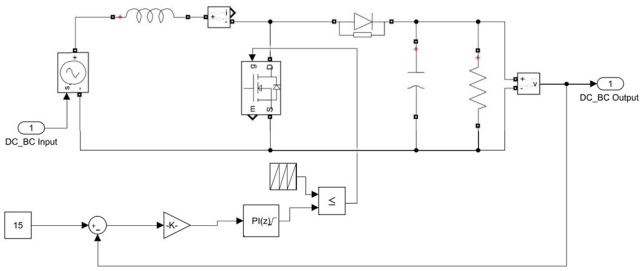


Fig. 6. The DC boost converter circuit.

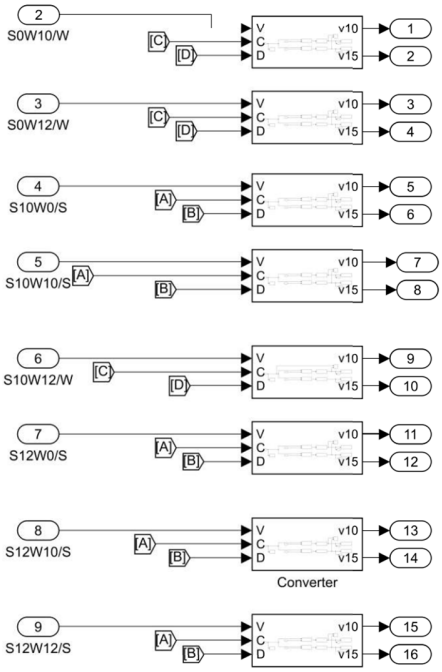


Fig. 7. DC to AC voltage output.

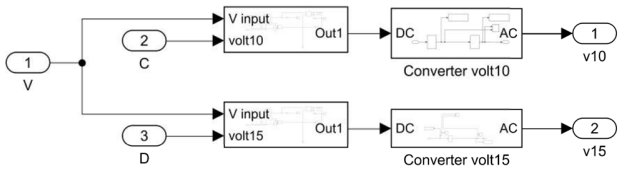


Fig. 8. DC boost converter and DC to AC inverter system.

The increased output voltage from the DC BC is supplied into Converter volt10 which is a DC to AC inverter. The inverter will invert the DC input voltage to an AC voltage which is used to supply to any connected LOAD.

## IV. RESULTS AND DISCUSSION

The proposed VBCC model was fully developed in Matlab/Simulink. Voltage sensing and measuring method was used to assist the controller in coordinating, switching, and effectively managing the respective tasks such as supplying the inverted DC voltage into AC for connected LOAD or boosting the DC voltage to perform charging on the battery energy system. At in the beginning of this paper, we used the condition S10W10 to depict the developed VBCC's system methodology. Thus, the condition S10W10 will also be used to present the results of each stage of the developed VBCC to validate the developed system's overall performance and to analyze the respective required generated signals.

### *A. Solar – Wind Renewable Energy Sources*

Figure 9 shows the solar - wind RESs input voltages captured based on the preset value shown in Figure 1. Hence, the 11V voltage captured is an amount of the voltage that the connected solar – wind RESs are producing. These voltages are then sent into the ESCC as shown in Figure 1. In the ESCC, these voltages are captured by the individual solar and wind stateflow chart shown in Figure 10. Hence, when the solar and wind stateflow condition charts capture the output voltages of the solar – wind RESs, a logic 1 is produced by each stateflow condition chart. Referring to Figure 10, solar and wind stateflow condition charts give a logic 1 for 11V sensed and measured voltage.

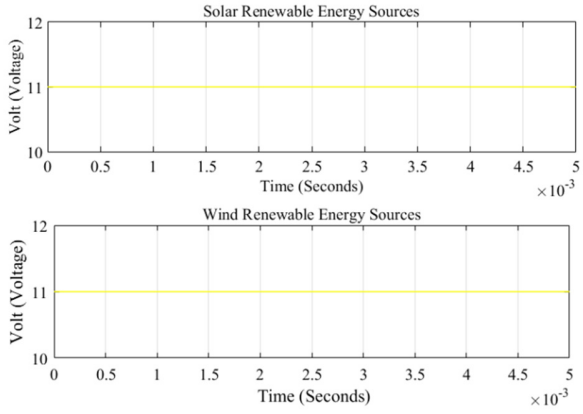


Fig. 9. Solar – wind RESs input voltages.

(a)

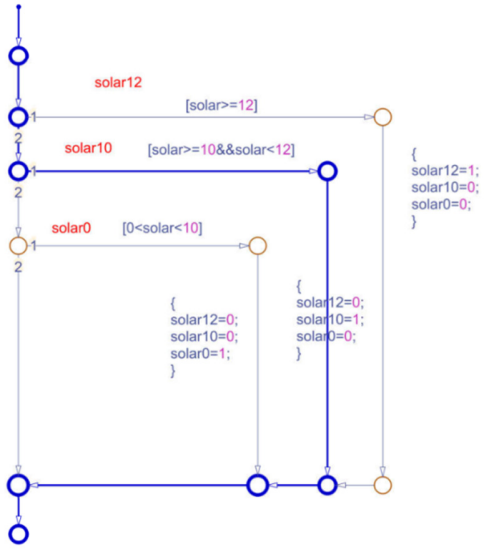


(b)

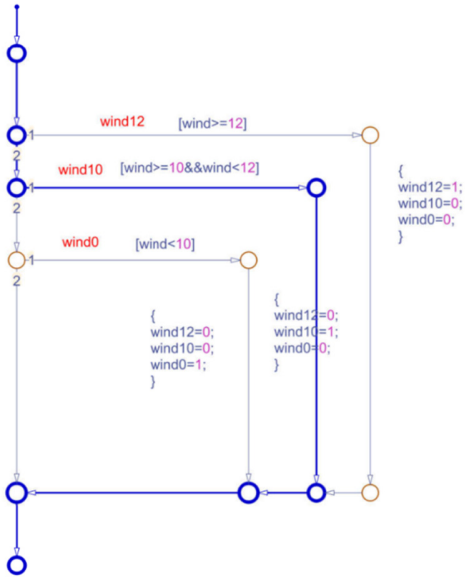


Fig. 10. 11V of solar – wind stateflow condition chart.

Both logics are sent into the electronic logic "AND" gate circuit through the ports solar10 and wind10 as shown in Figure 1. Figure 11 shows the solar10 and wind10 logic output based on the sensed and measured output voltage shown in Figure 10. The solar10 and wind10 logic 1 is sent into the AND gate LO6 shown in Figure 3 for an output of logic 1.

TABLE II. AND GATES COMBINATIONAL OUTPUT – S10W10

| AND gates combinations | Output |
|---|---|
| S0W0 | 0 |
| S0W10 | 0 |
| S0W12 | 0 |
| S10W0 | 0 |
| S10W10 | 1 |
| S10W12 | 0 |
| S12W0 | 0 |
| S12W10 | 0 |
| S12W12 | 0 |

Based on Table II, the combinational output of the S10W10 AND gates shown in Figure 3 is the logic 1. This S10W10 logic 1 is sent to the S10W10 port of electronic condition switching circuit as shown in Figure 1. The S10W10 logic 1 connects the port 7 S10W10 of the 9 Conditional Switching Circuits shown in Figure 4(a) to activate the S10W10 Condition Switching Circuit shown in Figure 4(b). The S10W10 logic 1 will switch the relays from NO to NC to allow the SOLAR Input 11V and WIND Input 11V to flow into port 1 (S10W10/S) and 2 (S10W10/W) as shown in Figure 4. Figure 12 shows the 11V voltage output captured at ports S10W10/S and S10W10/W as shown in Figure 4(a).

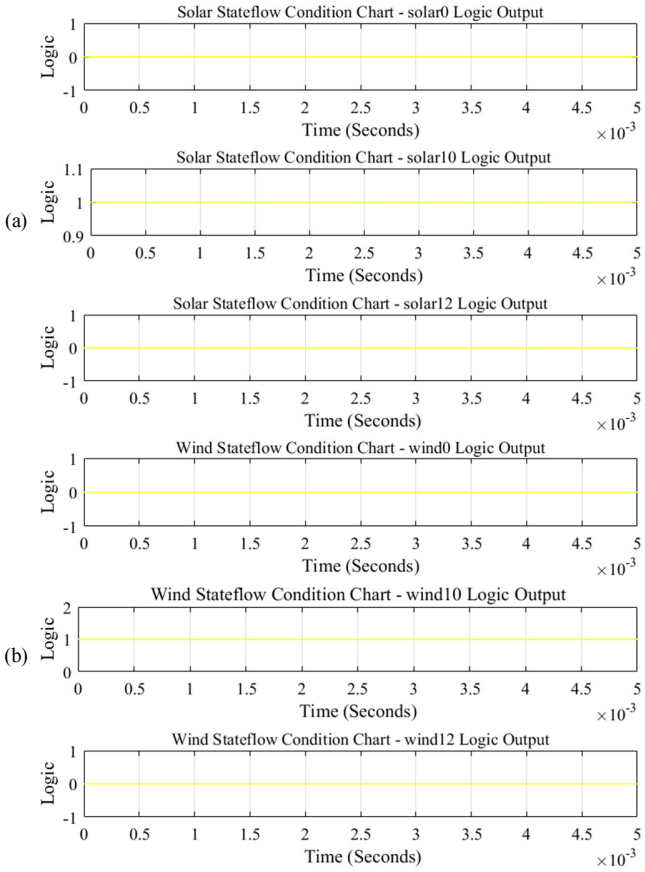


Fig. 11. Solar stateflow condition chart – (a) solar10 Logic Output and (b) wind10 Logic Output.

Referring to Figure 1, the 11V voltage at S10W10/S is connected to the current conversion circuit, while the 11V voltage at S10W10/W is connected to the DC BC. Figure 13 shows the input 11V voltage at S10W10/W – DC-BC Input and the approximately 16V voltage output at the DC_BC Output as shown in Figure 6. The 16V voltage output at the DC_BC Output is connected to the battery energy system as shown in Figure 5 to charge the batteries used as an energy storage system. Figure 14 shows the results captured when the 16V voltage output at the DC_BC Output is connected as input to the DC to AC Inverter. The 16V voltage is inverted into 240V AC Voltage Output at the DC to AC Inverter, which is then used to supply the connected load.

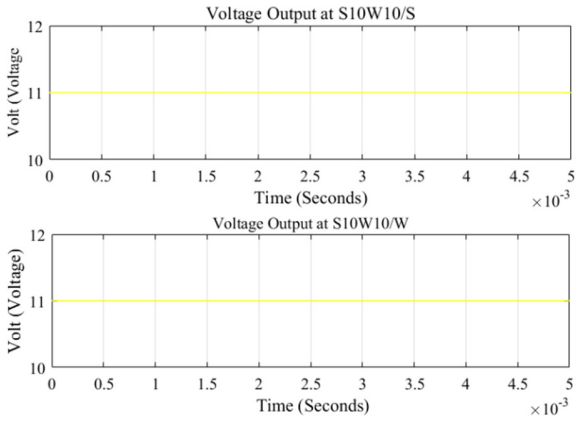


Fig. 12. Voltage output at S10W10/S and S10W10/W.

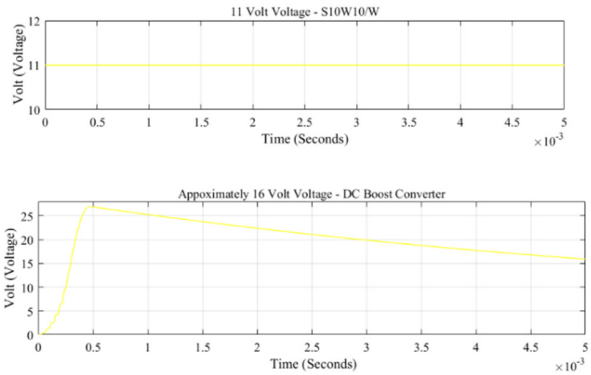


Fig. 13. Input and output voltage – DC boost converter.

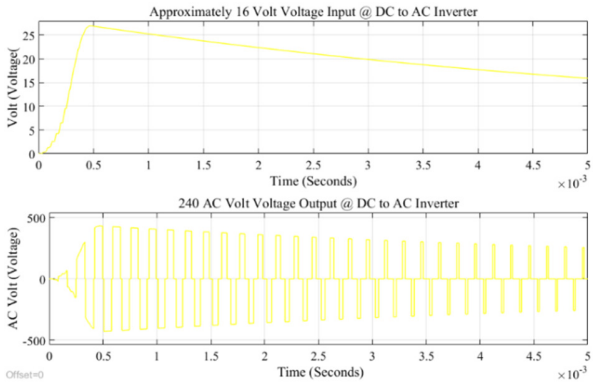


Fig. 14. 16V voltage input and 240V AC output at the DC to AC inverter.

The presented results are for condition S10W10, while the results for all the other conditions were compiled and are presented in Tables III and IV.

## V. CONCLUSION

Based on the presented literature review, a VBCC for solar – wind RES was proposed, modeled, and developed in this paper. The modeling and development of the VBCC was conducted in order to sense and measure the incoming voltages from the solar and wind RES. The other aims of VBCC are to coordinate, switch, and effectively manage the produced energy from the available voltages. The presented research

methodology has successfully developed the VBCC. The obtained results show that the developed VBCC can coordinate, switch, and effectively manage the available energy for connected load and battery energy system charging.

TABLE III. ESCC OUTPUT LOGIC CONDITIONS

| ESCC Output Logic Conditions | | | | | |
|---|---|---|---|---|---|
| **S0** | **S10** | **S12** | **W0** | **W10** | **W12** |
| 1 | | | 1 | | |
| 1 | | | | 1 | |
| 1 | | | | | 1 |
| | 1 | | 1 | | |
| | 1 | | | 1 | |
| | 1 | | | | 1 |
| | | 1 | 1 | | |
| | | 1 | | 1 | |
| | | 1 | | | 1 |

TABLE IV. ELGC COMBINATIONAL OUTPUT LOGICS

| ELGC Combinational Output Logics | | | | | | | | |
|---|---|---|---|---|---|---|---|---|
| **C9** | **C8** | **C7** | **C6** | **C5** | **C4** | **C3** | **C2** | **C12** |
| **S0W0** | **S0W10** | **S0W12** | **S10W0** | **S10W10** | **S10W12** | **S12W0** | **S12W10** | **S12W12** |
| 1 | | | | | | | | |
| | 1 | | | | | | | |
| | | 1 | | | | | | |
| | | | 1 | | | | | |
| | | | | 1 | | | | |
| | | | | | 1 | | | |
| | | | | | | 1 | | |
| | | | | | | | 1 | |
| | | | | | | | | 1 |

## ACKNOWLEDGMENT

The authors gratefully acknowledge the support by the Centre of Telecommunication Research & Innovation (CeTRI), Fakulti Kejuruteraan Elektronik dan Kejuruteraan Komputer (FKEKK), and Faculty of Mechanical and Manufacturing Engineering Technology (FTKMP), Universiti Teknikal Malaysia Melaka, and the Ministry of Higher Education, Malaysia. Also, the authors thank the Centre of Artificial Intelligence and Robotic iKohza Malaysia-Japan International Institute of Technology, Universiti Teknologi Malaysia (UTM).

## REFERENCES

[1] Md. S. Alam, F. S. Al-Ismail, A. Salem, and M. A. Abido, "High-Level Penetration of Renewable Energy Sources Into Grid Utility: Challenges and Solutions," *IEEE Access*, vol. 8, pp. 190277–190299, 2020, https://doi.org/10.1109/ACCESS.2020.3031481.

[2] Md. S. Alam, F. S. Al-Ismail, A. Salem, and M. A. Abido, "High-Level Penetration of Renewable Energy Sources Into Grid Utility: Challenges and Solutions," *IEEE Access*, vol. 8, pp. 190277–190299, 2020, https://doi.org/10.1109/ACCESS.2020.3031481.

[3] P. S. Gotekar, S. P. Muley, and D. P. Kothari, "A Single Phase Grid Connected PV System working in Different Modes," *Engineering, Technology & Applied Science Research*, vol. 10, no. 5, pp. 6374–6379, Oct. 2020, https://doi.org/10.48084/etasr.3746.

[4] Y. Kassem, H. Camur, and O. a. M. Abughinda, "Solar Energy Potential and Feasibility Study of a 10MW Grid-connected Solar Plant in Libya," *Engineering, Technology & Applied Science Research*, vol. 10, no. 4, pp. 5358–5366, Aug. 2020, https://doi.org/10.48084/etasr.3607.

[5] S. A. Dayo, S. H. Memon, M. A. Uqaili, and Z. A. Memon, "LVRT Enhancement of a Grid-tied PMSG-based Wind Farm using Static VAR Compensator," *Engineering, Technology & Applied Science Research*, vol. 11, no. 3, pp. 7146–7151, Jun. 2021, https://doi.org/10.48084/etasr.4147.

[6] A. Al-Quraan and M. Al-Qaisi, "Modelling, Design and Control of a Standalone Hybrid PV-Wind Micro-Grid System," *Energies*, vol. 14, no. 16, Jan. 2021, Art. no. 4849, https://doi.org/10.3390/en14164849.

[7] M. F. Zia, E. Elbouchikhi, and M. Benbouzid, "Microgrids energy management systems: A critical review on methods, solutions, and prospects," *Applied Energy*, vol. 222, pp. 1033–1055, Jul. 2018, https://doi.org/10.1016/j.apenergy.2018.04.103.

[8] A. Anvari-Moghaddam, A. Rahimi-Kian, M. S. Mirian, and J. M. Guerrero, "A multi-agent based energy management solution for integrated buildings and microgrid system," *Applied Energy*, vol. 203, pp. 41–56, Oct. 2017, https://doi.org/10.1016/j.apenergy.2017.06.007.

[9] C.-S. Karavas, G. Kyriakarakos, K. G. Arvanitis, and G. Papadakis, "A multi-agent decentralized energy management system based on distributed intelligence for the design and control of autonomous polygeneration microgrids," *Energy Conversion and Management*, vol. 103, pp. 166–179, Oct. 2015, https://doi.org/10.1016/j.enconman.2015.06.021.

[10] S.-H. Yoon, S.-Y. Kim, G.-H. Park, Y.-K. Kim, C.-H. Cho, and B.-H. Park, "Multiple power-based building energy management system for efficient management of building energy," *Sustainable Cities and Society*, vol. 42, pp. 462–470, Oct. 2018, https://doi.org/10.1016/j.scs.2018.08.008.

[11] P. Kofinas, A. I. Dounis, and G. A. Vouros, "Fuzzy Q-Learning for multi-agent decentralized energy management in microgrids," *Applied Energy*, vol. 219, pp. 53–67, Jun. 2018, https://doi.org/10.1016/j.apenergy.2018.03.017.

[12] W. Liu *et al.*, "Smart Micro-grid System with Wind/PV/Battery," *Energy Procedia*, vol. 152, pp. 1212–1217, Oct. 2018, https://doi.org/10.1016/j.egypro.2018.09.171.

[13] G. V. B. Kumar, P. Kaliannan, S. Padmanaban, J. B. Holm-Nielsen, and F. Blaabjerg, "Effective Management System for Solar PV Using Real-Time Data with Hybrid Energy Storage System," *Applied Sciences*, vol. 10, no. 3, Jan. 2020, Art. no. 1108, https://doi.org/10.3390/app10031108.

[14] O. O. Mengi and I. H. Altas, "A New Energy Management Technique for PV/Wind/Grid Renewable Energy System," *International Journal of Photoenergy*, vol. 2015, Mar. 2015, Art. no. e356930, https://doi.org/10.1155/2015/356930.

[15] A. M. Abdelshafy, J. Jurasz, H. Hassan, and A. M. Mohamed, "Optimized energy management strategy for grid connected double storage (pumped storage-battery) system powered by renewable energy resources," *Energy*, vol. 192, Feb. 2020, Art. no. 116615, https://doi.org/10.1016/j.energy.2019.116615.

[16] M. Chen, S. Ma, H. Wan, J. Wu, and Y. Jiang, "Distributed Control Strategy for DC Microgrids of Photovoltaic Energy Storage Systems in Off-Grid Operation," *Energies*, vol. 11, no. 10, Oct. 2018, Art. no. 2637, https://doi.org/10.3390/en11102637.

[17] Y. Salgueiro, M. Rivera, and G. Nápoles, "Multi-agent-Based Decision Support Systems in Smart Microgrids," in *Intelligent Decision Technologies 2019*, Singapore, 2020, pp. 123–132, https://doi.org/10.1007/978-981-13-8311-3_11.

[18] I. N. Moghaddam, "Optimal Sizing and Operation of Energy Storage Systems to Mitigate Intermittency of Renewable Energy Resources," Ph.D. dissertation, University of North Carolina at Charlotte, Charlotte, NC, USA, 2018.

[19] R. S. S. Singh, M. Abbod, and W. Balachandran, "Renewable energy resource self-intervention control technique using Simulink/Stateflow modeling," in *Proceedings of the 50th Universities Power Engineering Conference (UPEC 2015)*, Trent, UK, 2015, vol. 2015, https://doi.org/10.1109/UPEC.2015.7339803.